Molecular Crystals and Liquid Crystals
Publication details, including instructions for authors and subscription information:
http://www.tandfonline.com/loi/gmcl20

Double Peak Specific Heat Capacity Anomaly in Mixtures of Liquid Crystals and Nanoparticles

D. Jesenek [a], S. Kralj [a b], G. Cordoyiannis [a c] & Z. Kutnjak [a]

[a] Jožef Stefan Institute, Ljubljana, Slovenia

[b] Laboratory of Physics of Complex Systems, Faculty of Natural Sciences and Mathematics, University of Maribor, Maribor, Slovenia

[c] EN FIST Centre of Excellence, Ljubljana, Slovenia

Version of record first published: 16 Jun 2011

To cite this article: D. Jesenek, S. Kralj, G. Cordoyiannis & Z. Kutnjak (2011): Double Peak Specific Heat Capacity Anomaly in Mixtures of Liquid Crystals and Nanoparticles, Molecular Crystals and Liquid Crystals, 546:1, 3/[1473]-10/[1480]

To link to this article: http://dx.doi.org/10.1080/15421406.2011.571169

Mol. Cryst. Liq. Cryst., Vol. 546: pp. 3/[1473]–10/[1480], 2011

ISSN: 1542-1406 print/1563-5287 online
DOI: 10.1080/15421406.2011.571169

Taylor & Francis
Taylor & Francis Group

Double Peak Specific Heat Capacity Anomaly in Mixtures of Liquid Crystals and Nanoparticles

D. JESENEK,[1] S. KRALJ,[1,2] G. CORDOYIANNIS,[1,3] AND Z. KUTNJAK[1]

[1]Jožef Stefan Institute, Ljubljana, Slovenia
[2]Laboratory of Physics of Complex Systems, Faculty of Natural Sciences and Mathematics, University of Maribor, Maribor, Slovenia
[3]EN FIST Centre of Excellence, Ljubljana, Slovenia

The liquid crystal phase behaviour in the interval close to the isotropic-nematic phase transition and in the vicinity of wetting and dewetting interface has been analysed. For the theoretical study Landau-de Gennes mesoscopic model in terms of the tensor orientational order parameter has been used.

It has been shown that in an appropriate interval of surface wetting interaction strengths, wetting and dewetting phenomena could take place. This phenomenon could be a reason behind the observed double peak anomaly in the specific heat capacity C_p *temperature dependence in a mixture of nanoparticles and liquid crystals.*

Keywords Dewetting; double-peak anomaly; liquid crystal; mixtures; nanoparticles; wetting

1. Introduction

For several years there is an interest in surface-induced wetting and dewetting phenomena at a liquid crystal-confining substrate interface [1,2]. Such phenomena are of interest for several electro-optical applications. In addition, the corresponding physics shows several universalities. Consequently, the results obtained in liquid crystal (LC) systems are of interest also for other condensed matter systems.

Most of such investigations were performed in thermotropic LCs close to the isotropic-nematic (I-N) phase transition [3–5]. In these studies it was assumed that the surface wetting strength is linearly proportional to the uniaxial nematic order parameter S.

It has been shown that in an appropriate interval of surface wetting interaction strengths there might exists a discontinuous surface prewetting transition at a temperature T_S which is slightly above the bulk I-N phase transition temperature T_{IN}. Such phenomenon can also occur in mixtures of LCs and nanoparticles (NPs) at the LC-NPs interface. Therefore, this phenomenon could be a reason for a double

Address correspondence to D. Jesenek, Jožef Stefan Institute, Jamova 39, 1000 Ljubljana, Slovenia. Tel.: +386-1-4773447; Fax: +386-1-4773191; E-mail: dalija.jesenek@ijs.si

peak critical anomaly in the temperature dependence of the specific heat capacity C_p, which is commonly observed at the I-N phase transition [6–8].

In this paper we extend these studies to surface interactions which are proportional to different signs of the surface interaction strengths W and to a finite confinement cell thickness. We analyze the phase behaviour in order to find out if the wetting/dewetting phenomena can be the reason for the observed double peak anomaly. The plan of the paper is as follows; in Sec. II we present the theoretical background. The results are shown and discussed in Sec. III and summarized in the last section.

2. Theoretical Background

In order to study phenomena across the I-N phase transition, a Landau-de Gennes mesoscopic approach in terms of the tensorial order parameter $\underline{Q}$ has been used. The traceless symmetric tensor can be expressed as $\underline{Q} = \sum_{i=1}^{3} s_i \vec{e}_i \otimes \vec{e}_i$, where s_i stand for $\underline{Q}$-eigenvalues, $\vec{e}_i$ for $\underline{Q}$-eigenvectors, and $\otimes$ marks the tensor product operator. In case of local uniaxial order it can be expressed as $\underline{Q} = S\left(\vec{n} \otimes \vec{n} - \frac{\underline{I}}{3}\right)$, where $\underline{I}$ is the unit tensor, $\vec{n}$ is the unit vector and S is the uniaxial orientational order parameter. The so-called nematic director fieldpoints along a local uniaxial LC orientational ordering. The states $\pm\vec{n}$ are equivalent because of the head-to-tail equivalence of LC ordering at the mesoscopic level.

The free energy F of the system is given by $F = (f_c + f_e)d^3r + f_s d^2r$. The first (volume) integral is composed of the condensation (F_c) and elastic (f_e) free energy density contribution. The second (surface) integral introduces the interface free energy density f_s, describing the interactions at the LC-bounding substrate interface.

In the lowest order approximation we express the density contributions in terms of Q as

$$f_c = A_0(T - T_*)Q_{ij}Q_{ij} - BQ_{ij}Q_{jl}Q_{ji} + C\left(Q_{ij}Q_{ij}\right)^2, \tag{1a}$$

$$f_e = LQ_{ij,k}Q_{ij,k}, \tag{1b}$$

$$f_s = \frac{3}{2}We_i^{(s)}Q_{ij}e_j^{(s)}. \tag{1c}$$

Summations over repeated indices are assumed and $Q_{ij,k} = \frac{\partial Q_{ij}}{\partial x_k}$ stands for the partial derivative with respect to the Cartesian coordinate x_K. For bulk LC in thermodynamic limit the positive material constants A_0, B, C and T_* determine the degree of nematic ordering $S_b = \frac{B}{4C}\frac{3+\sqrt{9-8\frac{T-T_*}{T_{IN}-T_*}}}{4}$ in the bulk homogeneously aligned nematic phase below the bulk (I-N) phase transition temperature $T_{IN} = T_* + \frac{B^2}{24A_0C}$. Here T_* stands for the isotropic phase supercooling temperature. The elastic term penalizes the deviations from a spatially homogeneous ordering. Its relative strength is in the single elastic constant approximation given by the bare (independent of temperature) elastic constant L. The surface interaction term is represented by a single constant w and $\vec{e}^{(s)}$ stands for the interface normal vector. We have taken into account only the most essential terms needed to analyze surface phenomena of our interest.

The geometry of our problem is depicted in the inset of Figure 1. We consider a plane parallel cell, where cell plates are placed at $z = 0$ and $z = h$ of the Cartezian coordinate system (x, y, z). At $z = 0$ we impose the homeotropic anchoring condition given by Eq. (1(c)). At $z = h$ we set the free boundary condition.

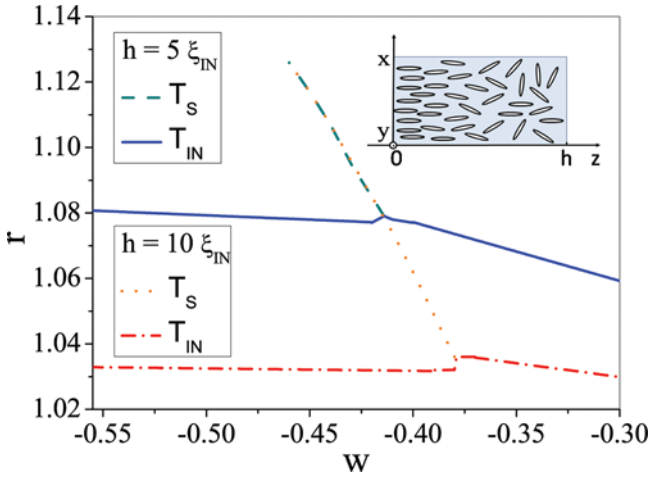

Figure 1. Phase diagram (r, w) for wetting conditions at cell thickness $h = 5\xi_0$ and $10\xi_0$. T_S and T_{IN} are surface and bulk transition temperatures, respectively. The inset shows the view of xy-plane in a plan parallel cell. The homeotropic anchoring is imposed at $z = 0$ and the free boundary condition is set at $z = h$.

Henceforth, we restrict to the uniaxial nematic ordering. We assume that in the nematic phase the director field is homogenously aligned along the z-axis and that $\underline{Q} = \underline{Q}(z)$. Consequently, the free energy density terms can be expressed as

$$f_c = a_0(T - T_*)S^2 - bS^3 + cS^4, \tag{2a}$$

$$f_e = L\left(\frac{\partial S}{\partial z}\right)^2, \tag{2b}$$

$$f_s = WS, \tag{2c}$$

where $a_0 = 2/3A_0$, $b = 2/9B$, $c = 4/9C$.

The characteristic sizes of the system are the nematic order parameter correlation length ξ and the surface extrapolation length d_e. They are both temperature dependent quantities. For the latter use we express them at the bulk I-N phase transition: $\xi_{IN} = \xi(T_{IN}) = \sqrt{\frac{L}{a_0(T_{IN} - T_*)}}$, $d_{IN} = d_e(T_{IN}) = \frac{LS_{IN}^2}{|W|S_{IN}}$, where $S_{IN} = S_b(T = T_{IN}) = b/(2C)$. We further introduce the scaled nematic order parameter $s = S/S_{IN}$ and the reduced temperature $r = (T - T_*)/(T_{IN} - T_*)$, and the dimensionless coordinate $\tilde{z} = z/h$. Using this scaling the dimensionless free energy $\tilde{F}$ is expressed as $\tilde{F} = \left(\int_0^1 rs^2 - 2s^3 + s^4 + \frac{\xi_{IN}^2}{h^2}\left(\frac{\partial s}{\partial \tilde{z}}\right)^2\right)d\tilde{z} + w\frac{\xi_{IN}}{h}s(\tilde{z} = 0)$, where $|w| = \xi_{IN}/d_{IN}$.

3. Results

The LC phase behaviour in the temperature interval above and below the bulk I-N phase transition temperature T_{IN} is considered. We focus on surface and bulk phase transitions by varying the surface interaction strength and the cell thickness h.

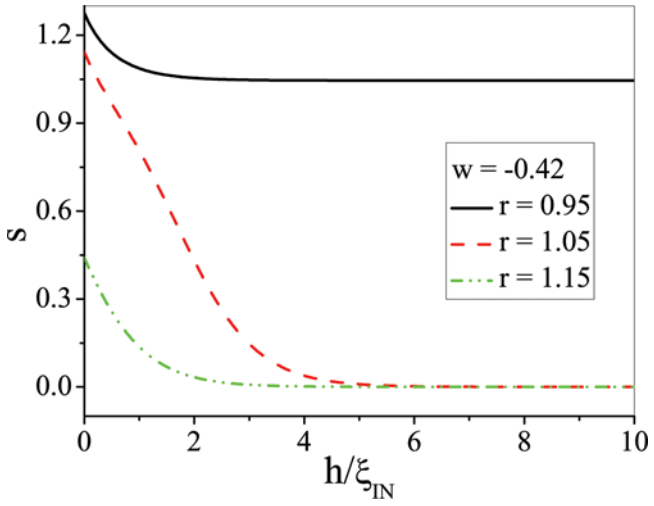

Figure 2. Variations of the scaled order parameter s as a function ofdistance to correlation length ratio h/ξ_0 away from the $z=0$ cell plate. Cell thickness is $h=10\xi_0$ and $w=-0.42$. At $r=0.95$ is first regime, at $r=1.05$ is second and at $r=1.15$ is third regime.

The phase behaviour for $w<0$ was already analyzed for a semi-infinite cell [3] and for a spherical confinement [4]. In this case, the surface promotes locally the nematic ordering. Our results, shown in Figure 1, match these results in the limit cases (i.e., $h->\infty$ in our simulations, results of ref. [3] and the radius is set to infinity in [4]). There are three qualitatively different regimes of behaviour on varying w, provided that h is much larger than ξ. The corresponding typical order parameter spatial variations are shown in Figure 2 and temperature variations in Figure 3. In the 1st regime, extending within the interval $|w| \in [0, w_1]$, only the bulk (I-N) phase transition exists at a temperature $T_{IN}(h) > T_{IN}$. With increasing $|w|$ the transition temperature slightly increases and the temperature shift is roughly linearly proportional to w. Because the surface potential promotes the nematic ordering, the order parameter exhibits a maximal value at the surface, which we label with $S_0 = S(z=0)$. Consequently, above $T_{IN}(h)$ the system exhibits a paranematic phase within the layer thickness comparable to the nematic correlation length. Within the 2nd regime, covering the interval $|w| \in [w_1, w_2]$, in addition to the bulk phase transition, a discontinuous surface phase transition takes place at a temperature $T_s(h) > T_{IN}(h)$. This temperature also increases roughly linearly with $|w|$ while $T_{IN}(h)$ remains essentially constant on varying w. The third regime extends above w_2. In this regime, the surface interaction is strong enough to dominantly influence the degree of surface ordering for all temperatures above $T_{IN}(h)$. Therefore, above the bulk transition temperature S_0 only gradually decreases on increasing T. Note that w_1 increases with h and saturates at a finite vale above $h \sim 10\xi$. On the other hand w_2 is roughly independent of h.

We next set $w>0$. The surface now promotes ordering with a negative uniaxiality ($S<0$), corresponding to an oblate average shape at the mesoscopic scale. The corresponding phase diagram is shown in Figure 4. Typical order parameter spatial profiles and temperature variations are shown in Figures 5 and 6, respectively. Again

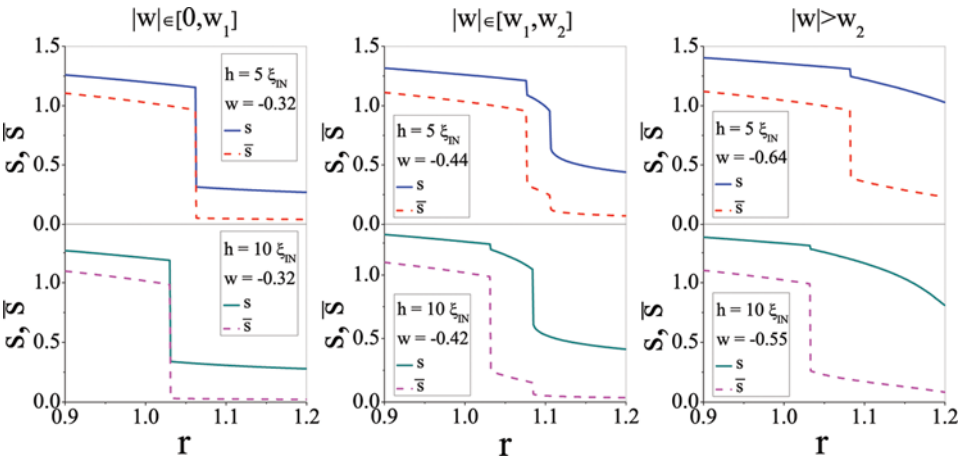

Figure 3. Variations of the scaled order parameter s and the average scaled order parameter $\bar{s}$ as a function of the reduced temperature r for wetting conditions. For cell thickness $h = 5\xi_0$ and $10\xi_0$ typical variations all three qualitatively different regimes are shown. (Figure appears in color online.)

the systems exhibit three qualitatively different regimes on increasing w. Nevertheless, in this case the surface tends to decrease the degree of ordering within the system which gives rise to a different topology of the phase diagram in the (w, T) plane. In the following we discuss the ordering changes on decreasing temperature from the isotropic phase. In the first regime ($w[0, w_1]$) only the bulk phase transition exists. The transition temperature T_{IN} roughly linearly decreases with increasing w. The order parameter now exhibits a lower value at the surface with respect to the ordering in the cell interior, see Figure 5. In the second regime, ($w \in [w_1, w_2]$) below the bulk phase transition, a discontinuous surface dewetting phase transition takes

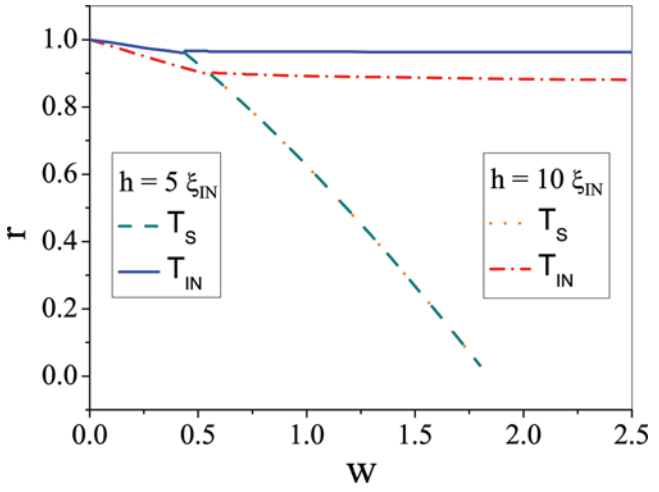

Figure 4. Phase diagram (r, w) for dewetting conditions at cell thickness $h = 5\xi_0$ and $10\xi_0$. T_S and T_{IN} are surface and bulk transition temperatures, respectively.

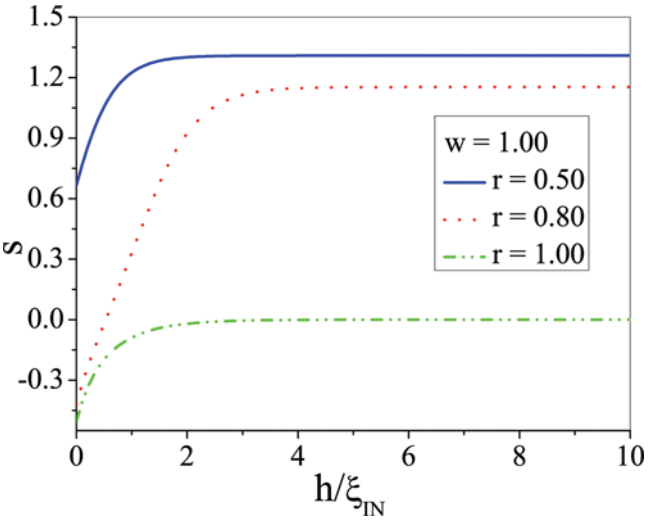

Figure 5. Variations of the scaled order parameter s as a function of distance to correlation length ratio h/ξ_0 away from the $z=0$ cell plate for $w=1.00$. At $r=0.50$ we have first regime, at $r=0.80$ is second and at $r=1.00$ is third regime. (Figure appears in color online.)

place. In this case, the surface degree of order parameter exhibits a discontinuous decrease below the surface dewetting transition temperature $T_S(h)$. The transition temperature apparently decreases linearly with respect to w. In the third regime ($w > w_2$) once again only the bulk transition exists.

In the following we analytically estimate the main topological features of the $(|w|, T)$ phase diagrams. Within the 1st regime it is sensible to assume that $s(0)$ is

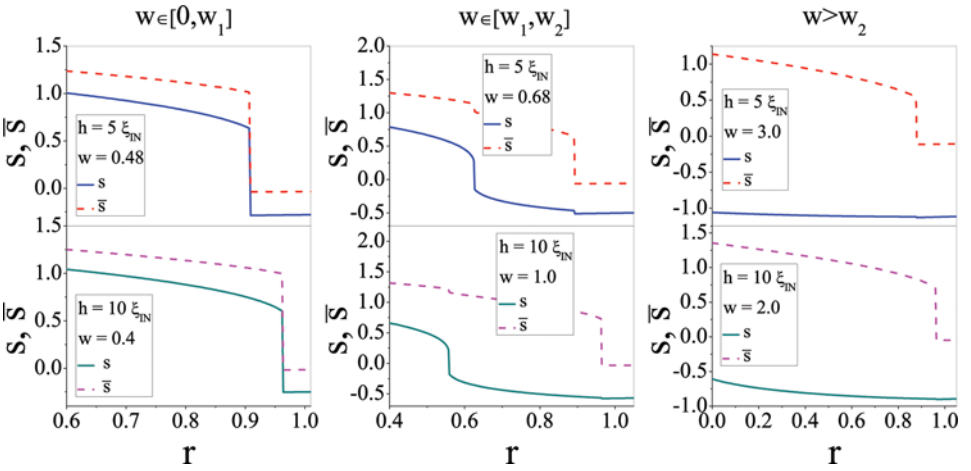

Figure 6. Variations of the scaled order parameter s and the average scaled order parameter $\bar{s}$ as a function of the reduced temperature r for dewetting conditions. For cell thickness $h = 5\xi_0$ and $10\xi_0$ typical variations all three qualitatively different regimes are shown. (Figure appears in color online.)

only slightly lifted and that the order in the remaining part of the cell follows it. The effective free energy can be then expressed as $\tilde{F}_{eff} \sim r\bar{s}^2 - \bar{s}^3 + \bar{s}^4 \pm \mu\bar{s}$, where $\mu = \frac{\xi_{IN}^2}{hd_{IN}} \approx |W|$ and $\bar{s}$ stands for the spatially averaged order parameter, $+\mu$ stands for $w > 0$ and $-\mu$ for $w < 0$. The bulk phase transition $T_{IN}(h)$ then takes place at the critical reduced temperature [9]

$$r_c = \frac{T_{IN}(h) - T_*}{T_{IN} - T_*} = 1 \mp \mu. \tag{3}$$

For $w < 0$ the Eq.(3) holds for $\mu < 0.5$. Note that the linear w dependence of r_c is clearly shown in Figure 1 and Figure 4.

In the regime II the surface interaction strength is strong enough to significantly increase $s(0)$ with respect to $\bar{s}$. We approximate the effective free energy of a thin surface layer and in the remaining part of the cell as us $<\tilde{F}_{eff}>_s \sim r\bar{s}^2 - \bar{s}^3 + \bar{s}^4 \pm \mu_{eff}\bar{s}$, where $\mu_{eff} \sim \frac{\xi_{IN}}{d_{IN}}$, and $<\tilde{F}_{eff}>_s \sim r\bar{s}^2 - \bar{s}^3 + \bar{s}^4$. Here $<\cdots>_s$ and $<\cdots>_V$ indicate the averages of the surface film of thickness ξ and within the remaining part of the cell, respectively. The free energy $<\tilde{F}_{eff}>_s$ determines the surface phase transition $T_S(h)$, which takes place at the reduced temperature $r_c^{(s)} = \frac{T_s(h) - T_*}{T_{IN} - T_*} \sim 1 \mp \mu_{eff}$. For $w < 0$ the equation is valid for $\mu_{eff} < 0.5$. For $\mu_{eff} > 0.5$ the noncritical behaviour of the surface prevails and, consequently, only gradual changes of the surface ordering are observed on varying temperature above $T_{IN}(h)$. The condition $\mu_{eff} = \frac{\xi_{IN}}{d_{IN}} = \frac{|w|\xi_{IN}}{L} = 0.5$ determines the critical surface interaction value $w = w_2$, where the second regime terminates for $w < 0$.

On the other hand, the bulk transition is dominantly governed by $<\tilde{F}_{eff}>_V$, yielding the critical reduced temperature $r_c^{(V)} = \frac{T_{IN}(h) - T_*}{T_{IN} - T_*} \sim 1$. The latter equation holds for $|w| > w_1$. These estimates well reproduce the main qualitative features observed in (T, $|w|$) phase diagrams shown in Figure 1 and Figure 4.

4. Conclusion

We have analyzed the LC behaviour in the vicinity of the interface, by varying the wetting and dewetting surface interaction strengths W as well as the distance from the interface. The present study has been performed near the I-N phase transition using a Landau-de Gennes mesoscopic model in terms of the tensor orientational order parameter.

It has been shown that, in a range of wetting and dewetting surface interaction strengths, the system exhibits two phase transitions between the I and N phases. Therefore, in an appropriate interval of the surface wetting or dewetting interaction strengths, wetting or dewetting phenomena can be the reason for the often observed double peak critical anomaly in the specific heat capacity C_p temperature dependence in a mixture of NPs and LCs [6]. In this case different values of h correspond to different concentration of NPs.

Acknowledgment

This work was supported by the Slovenian Research Agency under program P1-0099.

References

[1] Moses, T., & Shen, Y. R. (1991). *Phys. Rev. Lett.*, *67*, 2033.
[2] Fukuda, J. I., Stark, H., & Yokoyama, H. (2004). *Phys. Rev. E*, *69*, 021714.
[3] Sheng, P. (1982). *Phys. Rev. A*, *26*, 1610.
[4] Kralj, S., Žumer, S., & Allender, D. W. (1991). *Phys. Rev. A*, *43*, 2943.
[5] Sluckin, T. J., & Poniewierski, A. (1990), *Mol. Cryst. Liq. Cryst.*, *179*, 349.
[6] Mercuri, F., Paolini, S., Zammit, U., & Marinelli, M. (2005). *Phys. Rev. Lett.*, *94*, 247801.
[7] Yamamoto, J., & Tanaka, H. (2001). *Nature*, *409*, 321.
[8] Roshi, A., Iannacchione, G. S., Clegg, P. S., & Birgeneau, R. J. (2004). *Phys. Rev. E*, *69*, 031703.
[9] Cleaver, D. J., Kralj, S., Sluckin, T. J., & Allen, M. P. (1996). *The random anisotropy nematic spin model, Liquid Crystals in Complex Geometries formed by polymer and porous networks*, Crawford, G. P., Žumer, S. (Eds.), p. 467, Taylor and Francis: London.